50% EFFICIENT SOLAR CELL ARCHITECTURES AND DESIGNS

Allen Barnett[1], Christiana Honsberg[1], Douglas Kirkpatrick[2], Sarah Kurtz[3], Duncan Moore[4], David Salzman[5], Richard Schwartz[6], Jeffrey Gray[6], Stuart Bowden[1], Keith Goossen[1], Michael Haney[1], Dan Aiken[7], Mark Wanlass[3], Keith Emery[3]

[1]University of Delaware, [2]Defense Advanced Research Projects Agency (DARPA), [3]National Renewable Energy Laboratory (NREL), [4]University of Rochester, [5]LightSpin Technology, [6]Purdue University, [7]Emcore Corporation

ABSTRACT

Very High Efficiency Solar Cells (VHESC) for portable applications [1] that operate at greater than 55 percent efficiency in the laboratory and 50 percent in production are being created. We are integrating the optical design with the solar cell design, and have entered previously unoccupied design space that leads to a new paradigm. This project requires us to invent, develop and transfer to production these new solar cells. Our approach is driven by proven quantitative models for the solar cell design, the optical design and the integration of these designs. We start with a very high performance crystalline silicon solar cell platform. Examples will be presented. Initial solar cell device results are shown for devices fabricated in geometries designed for this VHESC Program.

INTRODUCTION

The realization of a high efficiency solar cell which is also manufacturable is the defining problem of photovoltaics. Our rigorous, model-driven approach overcomes limitations of existing approaches by developing an integrated optical and solar cell design which has efficiency greater than 55% at low concentration levels as well as multiple paths to low cost.

Our central innovation is to co-design the optical, interconnect and solar cell design, which dramatically increases the design space for high performance photovoltaics in terms of materials, device structures and manufacturing technology. This approach allows multiple benefits, including increased theoretical efficiency, new architectures which circumvent existing material/cost trade-offs, improved performance from non-ideal materials, device designs that can more closely approach ideal performance limits for existing solar technology (including silicon solar cells), reduced spectral mismatch losses and increased flexibility in material choices. An integrated optical/solar cell allows efficiency improvements while retaining low area costs, and hence expands the applications for photovoltaics. It allows a design approach which focuses first on performance, enabling the use of existing state-of-the-art photovoltaic technology to design high performance, low cost multiple junction III-Vs for the high and low energy photons and a new silicon solar cell for the mid-energy photons, all while circumventing existing cost drivers through novel solar cell architectures and optical elements.

LOW CONCENTRATION MULTIJUNCTIONS

A cornerstone of the integrated optical/electrical design is the use of low static concentration to realize several important advantages. The theoretical efficiency benefits of low concentration for high efficiency are shown in Figure 1. Since in practice the thermodynamic efficiency can typically not be achieved, we have used a "de-rating" factor of 0.8 for the ratio between an achievable efficiency and the thermodynamic efficiency. This means that in order to achieve >50%, the thermodynamic efficiency must exceed 63%. Figure 1 shows that low concentration (between 10X and 100X) reduces the number of required junctions from 9 to 5 junctions, and also shows that, because of the logarithmic dependence on the efficiency increase and concentration, the majority of the benefit from concentration is captured at low concentration ratios, for which the PV module is deployed like a flat plate module.

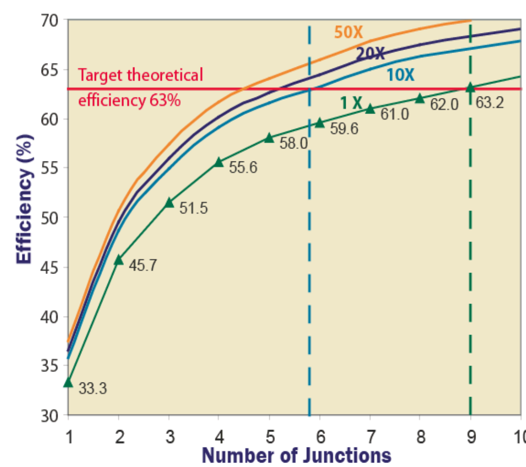

Figure 1: Theoretical efficiency as a function of concentration under AM1.5G conditions.

A second advantage of low concentration is the surface area not used for solar cells enables the design of novel integrated optical and solar cell architectures. There are two optical design and device architectures. The **Lateral Architecture** splits the light into spectral components, allowing individual devices to be optimized for each part of the spectrum. This design circumvents many material constraints by avoiding lattice and current matching and by eliminating spectral mismatch losses. The **Vertical Architecture** uses an independently contacted vertical junction stack, and realizes benefits similar to those of the lateral solar cell architecture. Each solar cell in a vertical stack can be independently contacted, thus avoiding current matching issues, increasing the flexibility in material choice and avoiding spectral mismatch.

Relaxing constraints related to lattice mismatch and series connection dramatically increases the ability to implement solar cells with ideal band gaps which are manufacturable and affordable. We propose to leverage the high performance and stability of existing best-practices solar cell technology while reducing costs. The program starts with highest-performance solar cell technologies and adds new device architectures and process technologies as they demonstrate **(1) higher performance** at a similar cost or **(2) lower cost** at the same performance. Every significant technical risk is addressed along diversified, competing paths to reduce risk. The flexibility of the architectures allows a wide portal to accommodate new breakthrough concepts such as nanotechnology and biologically-inspired materials for lower cost [2] as well as new high performance concepts.

Optimum band gaps for a 6J solar cell are shown in Figure 2, and demonstrate that the relaxation of series connection and lattice matching enables the development of the solar cell on a silicon platform. The Si platform provides many advantages, but importantly it is the only material capable of presently meeting both the efficiency target (in the wavelength range near its band gap) and the cost targets. The design also allows existing high performance materials to be used for two of the higher band gaps. A final advantage of low concentration is that the solar cell becomes less sensitive to defects, due to the increased operating point of the devices.

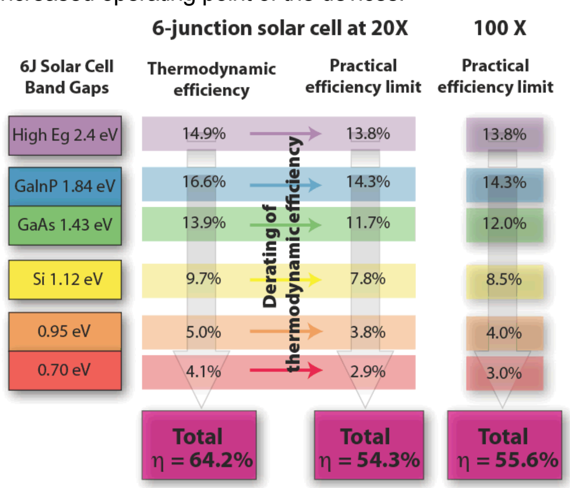

Figure 2: Band gaps for 6J solar cell.

INTEGRATED ARCHITECTURES: OPTICAL AND PV

A central novelty of our approach is an integrated optical and solar cell design. By integrating the optical design with the solar cell design, a much broader choice of materials is permitted, allowing high efficiency, the removal of many existing cost drivers, and enabling the inclusion of multiple other innovations. The key optical element is a static concentrator, which is then used in either a lateral or a vertical architecture. To achieve compact and robust packaging, all of our optical concentrator approaches will be of a tiled nature as shown in Figure 3, the design of which will depend on the co-optimization of the optics and cells to achieve maximum conversion efficiency.

Static Concentrators: A static concentrator increases the power density on the solar cell, but does not need tracking, and is deployed and used identically to a 1-sun solar module by using a wide acceptance-angle optical element (typically non-imaging), which accepts light from a large fraction of the sky. Unlike a tracking concentrator, a static concentrator is able to capture most of the diffuse light, which makes up ~10% of the incident power in the solar spectrum. The trade-off for the wider acceptance angle is a lower concentration [3]. If the application allows the module position to be manually adjusted at any point in the year, the maximum concentration increases. Depending on how long the module is to remain in a fixed position, the concentration can range from 10X to 200X.

Lateral Solar Cell Architecture: A key innovation allowed by the use of static concentrators is a lateral solar cell architecture. In the lateral solar cell architecture, additional optical elements are integrated with the static concentrator, to split the solar spectrum into its component colors [4]. Separate solar cells are placed under each color band, and each solar cell can be contacted separately. The lateral solar cell architecture increases the choice of materials for multiple junction solar cells, since it avoids lattice and current matching constraints. Further, since the devices do not need to be series connected, spectral mismatch losses are reduced. Finally, by contacting the individual solar cells with individual voltage busses, the need for tunnel junctions is avoided. Since each material requires unique tunnel contact metallurgy, eliminating tunnel junctions represents a substantial simplification.

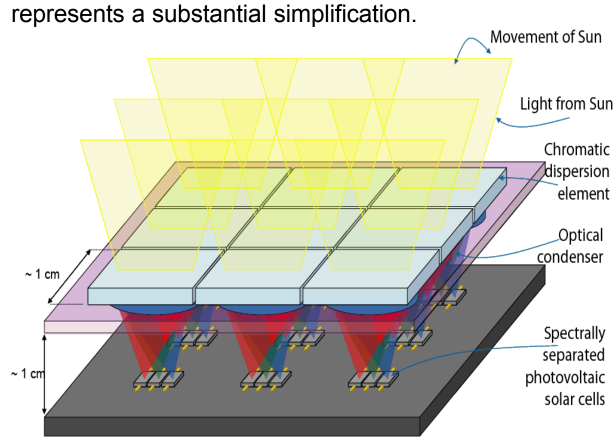

Figure 3: Schematic of the lateral solar cell approach.

The number of spectral regions or bins into which the spectrum is divided is determined by the optical design, with losses increasing as the number of spectral bins increases due to steering the sunlight onto the "wrong" solar cell (i.e., the high energy light falls on a solar cell with a low band gap). To circumvent this, a smaller number of individual solar cells, each consisting of 2 or 3 stacks, can be used. This corresponds to a hybrid of a vertical and lateral approach. In the solar cell device designs, we focus on dividing the light into three regions or bins – high energy, mid-energy and low energy as shown in Figure 4.

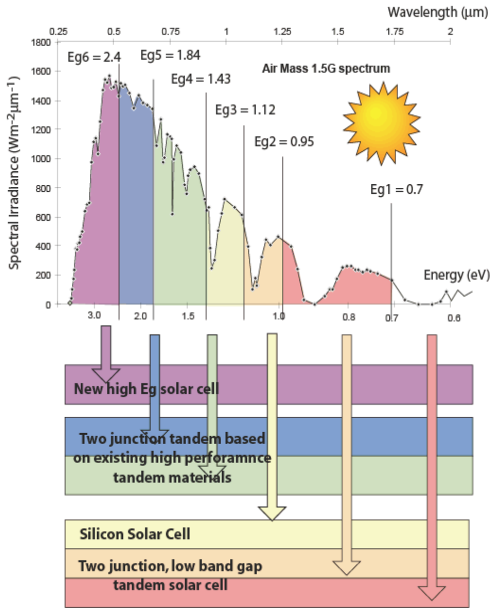

Figure 4: Schematic of the solar cell grouping for the lateral architecture.

Independently contacted vertical junction stack: A parallel approach to the lateral architecture is a vertically-integrated device in which the solar cells can be independently contacted. This approach is enabled due to the inclusion of static concentrators, which leave the majority of the surface area without an active solar cell, thus leaving room for separate contact formation to individual junctions. The independently-connected vertical architecture realizes similar benefits as a lateral solar cell architecture in minimizing spectral mismatch, increasing flexibility of material choices [5] and avoiding tunnel contacts. Depending on the integration process, this approach may also avoid lattice matching by using layer transfer.

OPTICAL DESIGNS

In the lateral configuration, a dispersive device is inserted in the optical path (like a diffraction grating or prism) and the light is spread out in angle in the same way as occurs in a spectrometer. Unlike a spectrometer where there is a slit and therefore the size of the source is very small in the direction of the dispersion, the sun subtends a total angle of ~0.5 degrees. This complicates the designs as is described below. Another method of dispersing the light is to use dichroic mirrors where some wavelengths are reflected at a surface and others are transmitted as shown in Figure 5. Commercial examples of dichroic mirrors are cold mirrors where visible light is reflected and infrared is transmitted. A dichroic system serves as the baseline design for the lateral approach. There are ongoing designs for the lateral optics, focusing on issues such as the choice between spherically and or cylindrically symmetric optics, the number of layers in the coating which are compatible with an affordable optical system, many optical designs have achieved over 90% optical efficiency.

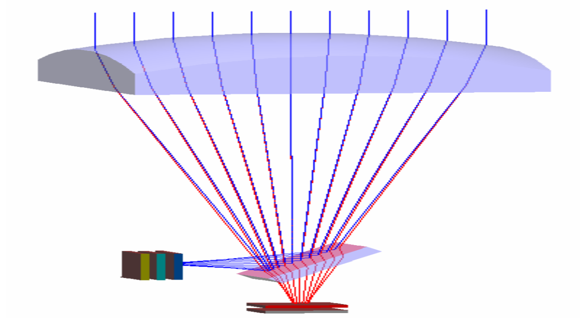

Figure 5: Schematic of the lateral optical system.

SOLAR CELL APPROACHES

The integrated optical/solar cell design removes the constraints of lattice and current matching, and hence allows integration of existing high performance technologies such as silicon, GaAs, and GaInP into a high performance device as shown in Figure 2 which has multiple paths to reduced cost. In addition, the development of a 6J tandem requires the development of additional devices and materials. One necessity is the need for high band gap solar cells, since an unconstrained optimized 6J solar cell has the top band gap at 2.4 eV. We utilize the increased flexibility of the design space to propose two other III-V based solar cells to achieve 2.1 eV or above, as well as the III-nitride material system for 2.4 eV solar cells. In addition, two low band gap junctions are needed, which can be implemented either by III-V materials (similar to those used in thermophovoltaic devices), or new approaches based on Ge and Si/Ge.

The flexibility of the optical/electrical design allows the incorporation of multiple types of solar cells, such as the combination of conventional semiconductors with nanostructured solar cells. We capitalize on this by developing nanostructured solar cells, both to address the potential for dramatically reduced cost, as well as to overcome the difficulties of achieving high voltage and efficiency from the low band gap stack. These approaches are described elsewhere [2].

COUPLED OPTICAL AND DEVICE MODELS

Detailed device models [6] are used throughout the program as a guide to optimum device designs under appropriate operating conditions. They are used to interpret diagnostic experiments, to predict the effects of proposed cell and system designs and to guide system choices. Appropriate levels of model sophistication are used. In some cases simple minority carrier diode models are sufficient; in others full detailed models which take into account heavy doping effects, degeneracy, graded band gaps, doping profiles, and other effects, not possible to include in simple minority carrier models, are used.

The device models are coupled to optical design tools. For example Figure 6 shows the effect of the changes in a dichroic mirror design upon the output power of a combination of a GaAs cell and a silicon cell where the dichroic mirror splits the spectrum in the vicinity of the GaAs band gap. Three cases are shown: an abrupt transition from transmission to reflection: a 100 nm transition; and a 200 nm transition. These results guide the choice of the location of the transition as well as the impact of changes in the location in the transition upon system performance. An additional benefit of the coupling of the optical and device models in this case is that it guides trade offs in the dichroic filter design. The sharper the transition required the great the number of layers required in the mirror and the higher the cost. Consideration of results like those of Figure 6 allows a trade between expense of the mirror and system efficiency.

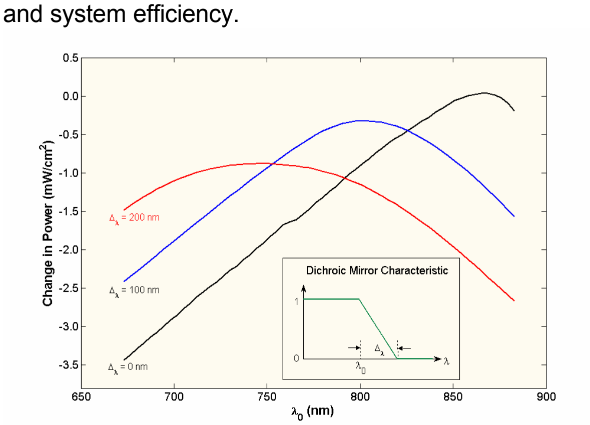

Figure 6: Change in power output relative to the power output with a dichroic mirror with an abrupt transition at the GaAs band edge (872 nm).

EFFICIENCY MEASUREMENT METHOD

The efficiency of a concentrator cell is usually measured without regard to the design or performance of the optics [7]. The efficiency of a lens-cell assembly reflects both the optical and cell efficiencies. No standard exists for characterization of the performance of a collection of concentrator cells designed for use under optics that split the spectrum into two or more parts. Consensus standards currently use a global reference spectrum for flat-plate measurements and a direct reference spectrum for concentrator measurements, but a reference spectrum for a low-concentration application has not been defined. Thus, cell performance measurements for the VHESC Program require two new elements: (1) definition of the spectrum relevant to this low concentration application and (2) identification of a methodology for quoting an aggregate efficiency for a set of cells that each use a different portion of the spectrum. These two issues have been addressed, respectively, by (1) choice of the AM1.5 Global spectrum [8], and (2) the solar spectrum is split, mathematically, either by defining dividing wavelengths or by any other method such that the spectral parts sum to give the one-sun reference spectrum. Each cell is then measured in the conventional way using the portion of the spectrum assigned to it. For the results presented here, the spectrum was divided into three sections with the GaInP/GaAs cell measured above the GaAs response (roughly 900 nm) and the GaInAsP/GaInAs cell with light beyond 1100 nm. The solar cells are measured over a range of concentrations, but the VHESC Program reporting conditions were taken as 20 suns.

The quantitative performance measurement of each individual solar cell uses reference cells to characterize the intensity of the solar simulator and a spectral mismatch correction factor to correct for differences between the test and reference cell responses and differences between the test and mathematically calculated reference spectrum relevant to that cell.

The most difficult measurement is for the low-band-gap series-connected tandem solar cell. Accurate measurement of this cell requires adjustment of the incident spectrum so that each of the junctions generates the correct photocurrent. Multisource simulators provide a means for obtaining the desired spectrum, but today's multi-source simulators do not achieve the concentrations desired for this project. For the low-band-gap tandem, a double-side polished silicon wafer was very helpful toward achieving the correct spectrum in both the multi-source and flash simulators.

Multi-junction solar cells based on all III-V compound series connected devices have achieved 37.9% efficiency at ~ 10 suns and 39% at 240 suns. Wanlass et. al. reported 37.9% at ~ 10 suns for a three-junction GaInP/GaAs/GaInAs cell grown in an inverted configuration [9]. This measurement of high efficiency at relatively low concentrations is consistent with those being pursued in the VHESC Program. King, et al, reported a 39% efficiency for a three-junction GaInP/Ga(In)As/Ge cell at 240 suns and an efficiency of 38.8% at 240 suns for a lattice-mismatched version of the same cell [10]. The 39% efficiency represents a fairly mature terrestrial concentrator version of the three-junction space cells. These concentrator cells are now commercially available with a typical efficiency >30% at 350 suns, demonstrating the progress this technology has made toward implementation in terrestrial solar applications.

INITIAL SOLAR CELL RESULTS

GaInP/GaAs tandem cells were prepared using trimethyl gallium, trimethyl indium, phosphine, arsine, and other precursors as described elsewhere [11]. These cells differ from conventional GaInP/GaAs cells because they transmit photons with energy less than 1.4 eV. An undoped GaAs wafer is used, and both the front and back contacts to the device are made on the front side (side with epilayer growth) of the GaAs wafer. This is possible because the active layers of the tandem cell are less than 5 μm thick. The cells use a second tunnel junction and a lateral n-type conduction layer to conduct the current from the back of the layer to the contact pad that forms a frame for the cell.

Light current-voltage (I-V) data are shown in Figure 7 for a GaInP/GaAs cell. An efficiency of 28.4% is seen at 20 suns concentration. The efficiency increases above 29% for concentrations above about 40 suns.

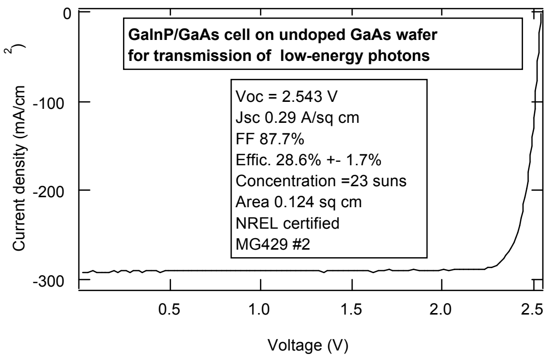

Figure 7: The light I-V curve for a GaInP/GaAs cell with both of the contacts accessible from the front side.

Lattice-matched, monolithic GaInAsP/GaInAs tandem solar cell structures grown on InP substrates are under development for the VHESC Program. The cell structures are grown by atmospheric-pressure metalorganic vapor-phase epitaxy at 620°C using conventional precursors. Series-connected, low-band-gap tandem cells were designed to operate at 20 suns concentration under the global spectrum truncated at a wavelength of 1100nm (i.e., our performance measurement convention for this device). Semi-realistic modeling studies show that the optimum subcell band gap pair is 0.95/0.74 eV if the bottom subcell is constrained to be GaInAs lattice-matched to InP. The subcells in the tandem structure are interconnected using a substantially transparent tunnel junction. The present devices are grown in an inverted fashion on IR-transparent (Fe) InP substrates to allow both contacts to be made on the back surface. The back contact is made to the back of the device mesa, and the front contact is made in the form of a frame around the mesa that contacts a highly conductive window layer on the front-surface of the device. The tandem is illuminated from the opposite side through the InP substrate. An efficiency of 3.5% at 5.7 suns without an anti-reflection coating represents an advanced stage of development for this new technology. The path to higher performance levels includes applying a good-quality, two-layer anti-reflection coating along with design revisions that will enable operation at higher concentration ratios. The assembled solar cell chips are shown in Figure 8.

SUMMARY

Solar cells with efficiency >50% allow a new functionality and new class of applications, but simultaneously require new approaches. We demonstrate that by finding a “sweet spot” for low concentration, we can achieve 50% with a realistic number of junctions, have closer match between ideal and practical efficiency and allow new optical/electrical integrated designs which circumvent current and lattice matching constraints.

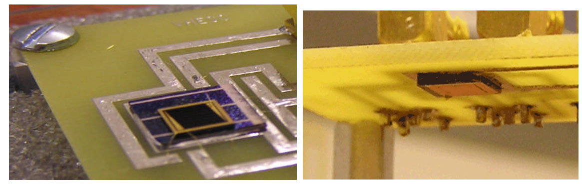

Figure 8: Photograph of the assembled solar cell chips.

ACKNOWLEDGEMENTS

This work was partially supported by DARPA/ARO Agreement No.: W911NF-05-9-0005. We thank Tom Moriarty, James Kiehl, S. Ward, J. Carapella, C. Kramer, M. Young, A. Duda, and C. Mack for the NREL sample preparation and measurement. NREL’s portion of this work was completed under Contract No. DE-AC36-99GO10337 with the U.S. Department of Energy.

REFERENCES

[1] D. Kirkpatrick, et al, this conference

[2] C. Honsberg, et al, this conference

[3] C. Minano, and A. Luque, “Limit of concentration under extended nonhomogeneous light sources,” *Applied Optics*, 22, 7, 2751-60, (1983).

[4] A. G. Imenes and D.R. Mills, “Spectral beam splitting technology for increased conversion efficiency in solar concentrating systems: a review,” *Solar Energy Materials & Solar Cells,* 84, 19-69, (2004).

[5] T. Trupke, and P. Wurfel, “Improved spectral robustness of triple tandem solar cells by combined series/parallel interconnection,” *Journal of Applied Physics*, 96, 4, 2347-51, (2004).

[6] S. M. Durbin and J. L. Gray, "Numerical Modeling of Photon Recycling in Solar Cells", IEEE Trans. Electron Devices, Vol. 41, No. 2, pp. 239-245, 1994.

[7] K. Emery, M. Meusel, R. Beckert, F. Dimroth, A. Bett and W. Warta, ”Procedures for Evaluating Multijunction Concentrators,” *Proc. 28th IEEE Photovoltaic Specialists Conf.*, Anchorage, AL, Sept. 15-22, 2000, pp. 1126-1130, IEEE, New York, 2000.)

[8] ASTM Standard G173, “Standard Tables for Reference Solar Spectral Irradiances: Direct Normal and Hemispherical on 37° Tilted Surface,” Amer. Society for Testing Matls., West Conshocken PA, USA

[9] M. W. Wanlass, S. P. Ahrenkiel, D. S. Albin, J. J. Carapella, A. Duda, K. Emery, J. F. Geisz, K. Jones, Sarah Kurtz, T. Moriarty, and M. J. Romero, "GaInP/GaAs/GaInAs Monolithic Tandem Cells for High-Performance Solar Concentrators," Proc. International Conference on Solar Concentrators for the Generation of Electricity or Hydrogen, May 1-5, 2005, Scottsdale, AZ, USA

[10] R. R. King, D. C. Law, C. M. Fetzer, et al., in *20th European Photovoltaic Solar Energy Conference*, Barcelona, Spain, 2005)

[11] K. A. Bertness, S. R. Kurtz, D. J. Friedman, et al., Appl Phys Lett **65**, 989 (1994).